JOURNAL OF GUIDANCE, CONTROL, AND DYNAMICS
Vol. 35, No. 1, January–February 2012

Reduced Balancing Transformations for Large Nonnormal State-Space Systems

Arthur C. Or,* Jason L. Speyer,† and John Kim‡
University of California, Los Angeles, Los Angeles, California 90095-1597

DOI: 10.2514/1.53777

Model reduction of nonnormal state-space input/output systems requires a dual-state (state and adjoint state) approach. With this approach the method of balanced truncation provides the baseline of reduced balanced transformation, allowing evaluation of other more numerically efficient forms of reduced balanced transformation that are obtained by direct methods. The shortcoming of balanced truncation is the numerical intractability to generate the full-order gramians and balanced transformation for large systems. In practice, reduced balanced transformation for large systems can be obtained from empirical-based methods using empirical-based gramians. Empirical model reductions methods include the well-known proper orthogonal decomposition, the balanced proper orthogonal decomposition, modified proper orthogonal decomposition, and pseudobalanced proper orthogonal decomposition. All are discussed in this paper. In our error analyses, the Karhunen–Loeve expansion based on proper orthogonal decomposition is extended to the generalized Karhunen–Loeve expansion based on balanced proper orthogonal decomposition, which is applicable for nonnormal systems. The error analyses highlight the importance of the dual-state-reduction approach. For model-reduction performance evaluation, the complex Orr–Sommerfeld input/output system is used.

I. Introduction

MODEL reduction of large linear time-invariant state-space input/output systems is of interest in modern control design. For flow control systems [1–4], reduced-order models allow lower-order filters and controllers to be used. It is well known that a similarity transformation can be obtained for balancing, that is, to achieve a simultaneous diagonalization of the controllability and observability gramians [5]. The method involves computing the two gramians by solving the exact equations [6]. The numerical problem of obtaining the full-order transformation can become intractable for large state-space systems. If the large similarity-transformation matrix is obtained, the columns and rows of its matrix inverse can be truncated according to the magnitude of the entries of the diagonal gramian. These entries are known as the Hankel singular values (HSVs). The resulting reduced-order transformation is called the baseline reduced balanced transformation (RBT). This analytical method is referred to as balanced truncation.

There are empirical-based methods to compute the gramians. There are direct methods to compute variant forms of the RBT. It is worthwhile to use balanced truncation [7,8] as a baseline for performance evaluation of the empirical and direct-method approaches [2,3,9,10]. In the next section we start with a brief introduction of balanced truncation and then show how a couple of variant forms of the RBT can be computed from direct methods. One method is based on the singular-value decomposition (SVD) published by Rowley [10]. The second method is developed by solving two eigenvalue problems involving the products of the gramians [2,11]. In the results the performance of the RBT can be evaluated against the analytical baseline.

The empirical gramian (controllability portion) is used in the well-known method of proper orthogonal decomposition (POD) [12]. Its singular values are related to the notion of modal "energy" ranking in the Karhunen–Loeve (KL) expansion [9], which forms the basis of error analysis for POD. We define the KL expansion as a special form of the least-squares method for reducing data. POD uses the resulting projectors from the KL expansion to produce a reduced-order model. Although POD is widely used, it is generally inadequate for reducing nonnormal input/output systems, which typically requires knowledge of the adjoint states [2,3,10]. For nonnormal input/output systems, a dual-state (state and adjoint state) reduction approach is essential. Rowley [10] extended POD to a balanced, dual-state version known as the balanced POD (BPOD), based on a SVD method of the RBT. In the error analyses, we extend the KL expansion to the generalized KL expansion, which shows the errors of BPOD. We also discuss two other types of model-reduction techniques. The modified POD, which uses a dual-state approach but is nonbalanced, is discussed. The reduced transformation used in the pseudobalanced POD (PBPOD), like POD, does not require the use of the adjoint state. But unlike POD, it achieves partial balancing. Both POD and PBPOD are motivated by model reductions of nonlinear systems, which does not possess state duality.

Finally, for numerical evaluation we choose the Orr–Sommerfeld (OS) system, which provides a good example of a nonnormal input/output state-space system. Certain interesting properties of nonnormal system behavior are discussed by the authors [4]. The OS system is complex, which is quite common in flow control stability problems. Since a detailed description of the OS system is available by the authors [2–4], the derivation will not be repeated here. Numerical results use the OS input/output system for performance evaluation throughout this paper. Matrix notations will be employed throughout the paper. All uppercase bold quantities represent matrices (with the exception of the input/output vectors). All row/column vectors are in lowercase bold. Subscripts mainly denote indices of a sequence; although it is used to convey meaning as well (such as c for controllability and o for observability). The paper is organized as the following. In Sec. II, the RBT forms are derived. Section III contains the error analysis. In Sec. IV, numerical results based on simulating the complex Orr–Sommerfeld system is presented. In Sec. V, we conclude the paper.

II. Reduced Balancing Transformations

A. Balanced Truncation Baseline

Consider a single-input single-output (SISO), complex state-space model with time-invariant elements:

Received 22 January 2011; revision received 3 July 2011; accepted for publication 6 July 2011.

*Research Associate, Mechanical and Aerospace Engineering Department. Senior Member AIAA.
†Professor, Mechanical and Aerospace Engineering Department. Fellow AIAA.
‡Professor, Mechanical and Aerospace Engineering Department. Associate Fellow AIAA.

$$\dot{\mathbf{x}} = \mathbf{A}\mathbf{x} + \mathbf{B}u, \qquad y = \mathbf{C}\mathbf{x} \tag{1}$$

where input signal $u(t)$ and output signal $y(t)$ are scalar functions, $\mathbf{A}$ is a $N \times N$ system matrix, $\mathbf{B}$ is a $N \times 1$ input vector and $\mathbf{C}$ is a $1 \times N$ output vector. If Eq. (1) is normal, that is, $\mathbf{A}\mathbf{A}^H = \mathbf{A}^H\mathbf{A}$ and $\mathbf{C} = \mathbf{B}^H$ (H denotes the conjugate/transpose), then one only needs to analyze Eq. (1) for model reduction. Otherwise, the dual form of Eq. (1) has to be considered as well:

$$\dot{\tilde{\mathbf{x}}} = \mathbf{A}^H\tilde{\mathbf{x}} + \mathbf{C}^H u^*, \qquad y^* = \mathbf{B}^H\tilde{\mathbf{x}} \tag{2}$$

where $*$ denotes the complex conjugate and $\tilde{\mathbf{x}}$ is the adjoint state vector. Both Eqs. (1) and (2) express the same input/output relationship and are equivalent to their corresponding complex transfer function. Note that $\tilde{\mathbf{x}}$ is in fact a complex conjugate variable because in the Laplace transform we require $\tilde{\mathbf{x}}(s^*) = \int_0^\infty \exp(-s^*t)\tilde{\mathbf{x}}(t)\,\mathrm{d}t$. In complex transfer function form, we have, respectively,

$$y/u = G(s) = \mathbf{C}(\mathbf{I}s - \mathbf{A})^{-1}\mathbf{B}$$
$$y^*/u^* = G^*(s^*) = \mathbf{B}^H(\mathbf{I}s^* - \mathbf{A}^H)^{-1}\mathbf{C}^H$$

The dynamics in Eq. (1) emphasizes controllability and the dynamics in Eq. (2) emphasizes observability. For balanced truncation, one seeks to balance the system with respect to the controllability and observability gramians, respectively,

$$\mathbf{G}_c = \int_0^\infty \exp(\mathbf{A}t)\mathbf{B}\mathbf{B}^H \exp(\mathbf{A}^H t)\,\mathrm{d}t$$
$$\mathbf{G}_o = \int_0^\infty \exp(\mathbf{A}^H t)\mathbf{C}^H\mathbf{C} \exp(\mathbf{A}t)\,\mathrm{d}t \tag{3}$$

For the two integrals exist, $\mathbf{A}$ only allows eigenvalues with negative real parts. By performing integration by parts on the integrals, it can be shown that the two gramians satisfy the following steady-state Lyapunov equations:

$$\mathbf{A}\,\mathbf{G}_c + \mathbf{G}_c\mathbf{A}^H + \mathbf{B}\mathbf{B}^H = \mathbf{0}, \qquad \mathbf{A}^H\mathbf{G}_o + \mathbf{G}_o\mathbf{A} + \mathbf{C}^H\mathbf{C} = \mathbf{0} \tag{4}$$

Efficient algorithms [6] exist to allow the $N \times N$ gramians to be computed. The algorithm can be extended to complex matrices. However, for large systems the algorithm is still a lot more computationally demanding than the empirical-based methods.

Once $\mathbf{G}_c$ and $\mathbf{G}_o$ are determined, one can obtain a similarity transformation $\mathbf{x}_b = \mathbf{T}\mathbf{x}$ (b denotes balanced), which simultaneously diagonalizes the two gramians. The relationship is governed by the following three full-order matrix equations:

$$\mathbf{G}_o\mathbf{T} = \mathbf{S}^H\mathbf{\Sigma}, \qquad \mathbf{G}_c\mathbf{S}^H = \mathbf{T}\mathbf{\Sigma}, \qquad \mathbf{S} = \mathbf{T}^{-1} \tag{5}$$

with three matrix unknowns, $\mathbf{T}$, $\mathbf{S}^H$, and $\mathbf{\Sigma}$. The diagonal matrix $\mathbf{\Sigma}$ contains ranked entries known as the HSVs. Once the similarity transformation is obtained, the baseline RBT can be obtained by performing row truncation on $\mathbf{S}$ and the same-order column truncation on $\mathbf{T}$, guided by the value of the HSVs. Therefore, the baseline RBT consists of $\mathbf{S}_1$ ($N_r \times N$) and $\mathbf{T}_1$ ($N \times N_r$), which are obtained from the first N_r rows of $\mathbf{S}$ and the first N_r columns of $\mathbf{T}$. To obtain the baseline RBT, one has to first determine the full-order similarity transformation.

The baseline balanced reduced-order model (ROM) ($N_r \times N_r$) is given by

$$\dot{\mathbf{x}}_r = \mathbf{A}_r\mathbf{x}_r + \mathbf{B}_r u, \qquad y = \mathbf{C}_r\mathbf{x} \tag{6}$$

where $\mathbf{A}_r = \mathbf{S}_1\mathbf{A}\mathbf{T}_1$, $\mathbf{B}_r = \mathbf{S}_1\mathbf{B}$, and $\mathbf{C}_r = \mathbf{C}\mathbf{T}_1$. The reduced-state vector and the original state vector are related by $\mathbf{x} = \mathbf{T}_1\mathbf{x}_r + \mathbf{e}$ and $\mathbf{x}_r = \mathbf{S}_1\mathbf{x}$. Likewise, the reduced-order adjoint system is given by

$$\dot{\tilde{\mathbf{x}}}_r = \mathbf{A}_r^H\tilde{\mathbf{x}}_r + \mathbf{C}_r^H u^*, \qquad y^* = \mathbf{B}_r^H\tilde{\mathbf{x}}_r \tag{7}$$

where $\tilde{\mathbf{x}} = \mathbf{S}_1^H\tilde{\mathbf{x}}_r + \tilde{\mathbf{e}}$ and $\tilde{\mathbf{x}}_r = \mathbf{T}_1^H\tilde{\mathbf{x}}$. Note that both error terms $\mathbf{e}$ and $\tilde{\mathbf{e}}$ are small in order that the ROM and the adjoint ROM are good approximations to their full-order systems. For the theory of the balancing transformation, we refer readers to Chen [5], Moore [7], Laub et al. [8], and Lall et al. [9].

B. Variant Forms of RBTs

For large state-space systems (those typically obtained by numerical discretization of linear partial differential systems), it is of interest to determine RBTs by direct methods, without first having to balance the full-order system.

The reduced-order version of Eqs. (5) gives the following set of reduced balancing equations:

$$\mathbf{G}_o\mathbf{T}_1 = \mathbf{S}_1^H\mathbf{\Sigma}_1, \qquad \mathbf{G}_c\mathbf{S}_1^H = \mathbf{T}_1\mathbf{\Sigma}_1, \qquad \mathbf{S}_1\mathbf{T}_1 = \mathbf{I} \tag{8}$$

where Eqs. (8) provide three matrix equations for three matrix unknowns, $\mathbf{S}_1$ ($N_r \times N$), $\mathbf{T}_1$ ($N \times N_r$) and $\mathbf{\Sigma}_1$ (diagonal, $N_r \times N_r$). The direct-method RBT is the solution of the unknowns $\mathbf{S}_1$ and $\mathbf{T}_1$.

To demonstrate the equivalence between the baseline RBT and the direct-method RBT, we compare the two sets of Eqs. (5) and (8). We partition the transformation matrices as

$$\mathbf{S} = \begin{bmatrix} \mathbf{S}_1 \\ \tilde{\mathbf{S}} \end{bmatrix}, \qquad \mathbf{T} = [\mathbf{T}_1 \quad \tilde{\mathbf{T}}] \tag{9}$$

For convenience and without confusion, the tilde notation, first introduced for the adjoint variables, is also used here to represent residual quantities. Substituting in Eqs. (5), the first two matrix equations yield

$$\mathbf{G}_o\mathbf{T}_1 = \mathbf{S}_1^H\mathbf{\Sigma}_1, \qquad \mathbf{G}_c\mathbf{S}_1^H = \mathbf{T}_1\mathbf{\Sigma}_1$$
$$\mathbf{G}_o\tilde{\mathbf{T}} = \tilde{\mathbf{S}}^H\tilde{\mathbf{\Sigma}}, \qquad \mathbf{G}_c\tilde{\mathbf{S}}^H = \tilde{\mathbf{T}}\,\tilde{\mathbf{\Sigma}} \tag{10}$$

The first two matrix equations above correspond to the first two of Eqs. (8). The third matrix equations (5) gives five constraint equations. These are

$$\mathbf{S}_1\mathbf{T}_1 = \mathbf{I}, \qquad \mathbf{S}_1\tilde{\mathbf{T}} = \mathbf{0}, \qquad \tilde{\mathbf{S}}\mathbf{T}_1 = \mathbf{0}$$
$$\tilde{\mathbf{S}}\,\tilde{\mathbf{T}} = \mathbf{I}, \qquad \mathbf{T}_1\mathbf{S}_1 + \tilde{\mathbf{T}}\tilde{\mathbf{S}} = \mathbf{I} \tag{11}$$

The first of Eqs. (11) is the same as the last of Eqs. (8). So we conclude that both Eqs. (5) and (8) determine the same solution for $\mathbf{S}_1$ and $\mathbf{T}_1$. The second, third and fourth matrix equations of Eq. (11) determine the residual transformations $\tilde{\mathbf{S}}$ and $\tilde{\mathbf{T}}$ (truncated portion).

In the next section, we address the question of errors caused by truncating $\tilde{\mathbf{S}}$ and $\tilde{\mathbf{T}}$. Rowley [10] pointed out that the orthogonality conditions between the RBT and its residual, that is, $\mathbf{S}_1\tilde{\mathbf{T}} = \mathbf{0}$ and $\tilde{\mathbf{S}}\mathbf{T}_1 = \mathbf{0}$, are crucial to balancing. Although these orthogonality conditions are part of the constraint [second and third matrix equations (11)], it can be shown that they are properties independent of the constraint equation. Based on the orthogonality properties between eigenvectors and their adjoint eigenvectors [see Eqs. (13) and the paragraph that follows below], one can establish these orthogonality conditions independently.

Here, two approaches for solving Eqs. (8) are considered. One is by an eigenvector method given in Sec. II.B.1 and the other is by SVD method given in Sec. II.B.2. The well-known SVD method was developed by Rowley [10]. We first establish the RBT performance based on exact gramians. For empirical studies we derive RBT based on the snapshot-based empirical gramians.

1. *Reduced Balancing Transformations by the Eigenvector Method*

Equation (8) yields two eigenvalue problems,

$$\mathbf{G}_c\mathbf{G}_o\mathbf{T}_1 = \mathbf{T}_1\mathbf{\Sigma}_1^2, \qquad \mathbf{G}_o\mathbf{G}_c\mathbf{S}_1^H = \mathbf{S}_1^H\mathbf{\Sigma}_1^2 \tag{12}$$

subject to a single constraint relationship $\mathbf{S}_1\mathbf{T}_1 = \mathbf{I}$. The significance of the products of gramians and their eigenvectors was pointed out by Safonov and Chiang [11], who considered real systems and used the Schur method to decompose the products to improve accuracy

potentially introduced by the ill-conditioned matrices. Consider an analogous example involving products of matrices. From SVD, we have $\mathbf{A} = \mathbf{U}_a \mathbf{\Lambda}_a \mathbf{V}_a^H$, where $\mathbf{U}_a$ and $\mathbf{V}_a$ are different if $\mathbf{A}$ is nonnormal. It can be shown that the columns of $\mathbf{U}_a$ and $\mathbf{V}_a$ are eigenvectors of the products $\mathbf{A}\mathbf{A}^H$ and $\mathbf{A}^H\mathbf{A}$, respectively. We have $\mathbf{A}\mathbf{A}^H\mathbf{U}_a = \mathbf{U}_a\mathbf{\Lambda}_a^2$ and $\mathbf{A}^H\mathbf{A}\mathbf{V}_a = \mathbf{V}_a\mathbf{\Lambda}_a^2$.

By conventional eigenvalue routines, we obtain

$$\mathbf{G}_c\mathbf{G}_o\mathbf{F}_1 = \mathbf{F}_1\mathbf{\Sigma}_1^2, \qquad \mathbf{G}_o\mathbf{G}_c\mathbf{E}_1 = \mathbf{E}_1\mathbf{\Sigma}_1^2 \tag{13}$$

where the eigenvectors in $\mathbf{E}_1$ and $\mathbf{F}_1$ are typically normalized in the decomposition. However, the constraint equation $\mathbf{S}_1\mathbf{T}_1 = \mathbf{I}$ cannot be satisfied in general by letting $\mathbf{S}_1 = \mathbf{E}_1^H$ and $\mathbf{T}_1 = \mathbf{F}_1$. Since $\mathbf{G}_c\mathbf{G}_o$ is the conjugate/transpose of $\mathbf{G}_o\mathbf{G}_c$, the matrix $\mathbf{F}_1^H\mathbf{E}_1$ and its conjugate/transpose $\mathbf{E}_1^H\mathbf{F}_1$ are diagonal.

To determine $\mathbf{S}_1$ and $\mathbf{T}_1$ we let $\mathbf{T}_1 = \mathbf{F}_1\mathbf{D}_t$ and $\mathbf{S}_1^H = \mathbf{E}_1\mathbf{D}_s$, where $\mathbf{D}_t$ and $\mathbf{D}_s$ are diagonal matrices used to supply the scalar weighting factors to the eigenvectors to satisfy the constraint. Substituting in Eqs. (8), we have to solve for $\mathbf{D}_t$ and $\mathbf{D}_s$ from the three equations:

$$\mathbf{G}_o\mathbf{F}_1\mathbf{D}_t = \mathbf{E}_1\mathbf{D}_s\mathbf{\Sigma}_1, \qquad \mathbf{G}_c\mathbf{E}_1\mathbf{D}_s = \mathbf{F}_1\mathbf{D}_t\mathbf{\Sigma}_1$$
$$\mathbf{D}_s^H\mathbf{E}_1^H\mathbf{F}_1\mathbf{D}_t = \mathbf{I} \tag{14}$$

It is convenient to separate the diagonal matrices into real amplitudes and phase angles, that is, $\mathbf{F}_1^H\mathbf{E}_1 = \mathbf{\Lambda}\exp(i\mathbf{\Theta})$, $\mathbf{D}_t = |\mathbf{D}_t|\exp(i\mathbf{\Theta}_t)$, and $\mathbf{D}_s = |\mathbf{D}_s|\exp(i\mathbf{\Theta}_s)$, where the notation $|.|$ represents the magnitudes of the diagonal entries. We multiply the first and second equations in Eq. (14) by $\mathbf{F}_1^H$ and $\mathbf{E}_1^H$, respectively, and substitute the amplitude-phase relationship, then Eq. (14) becomes

$$(\mathbf{F}_1^H\mathbf{G}_o\mathbf{F}_1)|\mathbf{D}_t|\exp(i\mathbf{\Theta}_t) = \mathbf{\Lambda}\exp(i\mathbf{\Theta})|\mathbf{D}_s|\exp(i\mathbf{\Theta}_s)\mathbf{\Sigma}_1 \tag{15}$$

$$(\mathbf{E}_1^H\mathbf{G}_c\mathbf{E}_1)|\mathbf{D}_s|\exp(i\mathbf{\Theta}_s) = \mathbf{\Lambda}\exp(-i\mathbf{\Theta})|\mathbf{D}_t|\exp(i\mathbf{\Theta}_t)\mathbf{\Sigma}_1 \tag{16}$$

$$|\mathbf{D}_s|\exp(-i\mathbf{\Theta}_s)\mathbf{\Lambda}\exp(-i\mathbf{\Theta})|\mathbf{D}_t|\exp(i\mathbf{\Theta}_t) = \mathbf{I} \tag{17}$$

All the matrices in the above equations, including $\mathbf{E}_1^H\mathbf{G}_c\mathbf{E}_1$ and $\mathbf{F}_1^H\mathbf{G}_o\mathbf{F}_1$, are diagonal; therefore, their products commute.

By eliminating $\mathbf{\Lambda}$ in the first two equations using the third equation, we determine the amplitude matrices to be

$$|\mathbf{D}_t| = (\mathbf{\Sigma}_1(\mathbf{F}_1^H\mathbf{G}_o\mathbf{F}_1)^{-1})^{1/2}, \qquad |\mathbf{D}_s| = (\mathbf{\Sigma}_1(\mathbf{E}_1^H\mathbf{G}_c\mathbf{E}_1)^{-1})^{1/2} \tag{18}$$

The phase equation is given by

$$\mathbf{\Theta}_t - \mathbf{\Theta}_s = \mathbf{\Theta} \tag{19}$$

This equation leaves the absolute phase angles undetermined. In this study, we let $\mathbf{\Theta}_s = \mathbf{0}$ and $\mathbf{\Theta}_t = \mathbf{\Theta}$. Finally, we have

$$\mathbf{T}_1 = \mathbf{F}_1|\mathbf{D}_t|\exp(i\mathbf{\Theta}), \qquad \mathbf{S}_1^H = \mathbf{E}_1|\mathbf{D}_s| \tag{20}$$

where $|\mathbf{D}_t|$ and $|\mathbf{D}_s|$ are given by Eq. (18). In the complex case, the RBT is not uniquely determined because of an arbitrary phase factor.

2. *Reduced Balancing Transformations by the SVD Method*

The SVD method described here is extracted from BPOD, with its snapshot-based data blocks replaced here by data blocks decomposed using exact gramians. The exact version of data blocks, $\mathbf{X}$ and $\mathbf{Y}$, are generated by

$$\mathbf{G}_c = \mathbf{U}_c\mathbf{\Sigma}_c\mathbf{U}_c^H = \mathbf{X}\mathbf{X}^H, \qquad \mathbf{G}_o = \mathbf{U}_o\mathbf{\Sigma}_o\mathbf{U}_o^H = \mathbf{Y}\mathbf{Y}^H \tag{21}$$

Therefore, we have

$$\mathbf{X} = \mathbf{U}_c\mathbf{\Sigma}_c^{1/2}, \qquad \mathbf{Y} = \mathbf{U}_o\mathbf{\Sigma}_o^{1/2}, \qquad \mathbf{H} = \mathbf{Y}^H\mathbf{X} \tag{22}$$

The matrix $\mathbf{H}$ is known as the generalized Hankel matrix.

Equations (8) can be rewritten as

$$\mathbf{Y}\mathbf{Y}^H\mathbf{T}_1 = \mathbf{S}_1^H\mathbf{\Sigma}_1, \qquad \mathbf{X}\mathbf{X}^H\mathbf{S}_1^H = \mathbf{T}_1\mathbf{\Sigma}_1, \qquad \mathbf{S}_1\mathbf{T}_1 = \mathbf{I} \tag{23}$$

The above form of the equations, by inspection, suggests that the solution is $\mathbf{S}_1^H = \mathbf{Y}\mathbf{M}_s$ and $\mathbf{T}_1 = \mathbf{X}\mathbf{M}_t$. Both $\mathbf{M}_s$ and $\mathbf{M}_t$ are square weighting matrices ($N_r \times N_r$). Substituting the two expressions into Eq. (8) gives a set of N_r^{th}-order matrix equations for $\mathbf{M}_t$ and $\mathbf{M}_s$:

$$\mathbf{H}\mathbf{M}_t = \mathbf{M}_s\mathbf{\Sigma}_1, \qquad \mathbf{H}^H\mathbf{M}_s = \mathbf{M}_t\mathbf{\Sigma}_1, \qquad \mathbf{M}_s^H\mathbf{H}\mathbf{M}_t = \mathbf{I} \tag{24}$$

The SVD of $\mathbf{H}$ produces $\mathbf{H} \approx \mathbf{U}_1\mathbf{\Lambda}_1\mathbf{V}_1^H$. Substituting $\mathbf{H}$ by its SVD form into Eqs. (24), we immediately note that the three equations with three unknowns are solved by letting

$$\mathbf{\Lambda}_1 = \mathbf{\Sigma}_1, \qquad \mathbf{M}_s = \mathbf{U}_1\mathbf{\Sigma}_1^{-1/2}, \qquad \mathbf{M}_t = \mathbf{V}_1\mathbf{\Sigma}_1^{-1/2} \tag{25}$$

Identities $\mathbf{U}_1^H\mathbf{U}_1 = \mathbf{V}_1^H\mathbf{V}_1$ are used. The first equation in Eqs. (25) indicates that the singular values of $\mathbf{H}$ are equal to the HSVs (diagonal entries of the balanced gramians). In the same form as derived by Rowley [10], the RBT becomes

$$\mathbf{S}_1 = \mathbf{M}_s^H\mathbf{Y}^H = \mathbf{\Sigma}_1^{-1/2}\mathbf{U}_1^H\mathbf{Y}^H, \qquad \mathbf{T}_1 = \mathbf{X}\mathbf{M}_t = \mathbf{X}\mathbf{V}_1\mathbf{\Sigma}_1^{-1/2} \tag{26}$$

Equations (26) of the SVD method and Eqs. (20) of the eigenvector method are two variant forms of RBT.

To see how the product of gramians relate to $\mathbf{H}$ of the SVD method, we note that

$$\mathbf{G}_c\mathbf{G}_o = \mathbf{X}(\mathbf{X}^H\mathbf{Y})\mathbf{Y}^H = \mathbf{X}\mathbf{H}^H\mathbf{Y}^H = \mathbf{X}(\mathbf{V}_1\mathbf{\Lambda}_1\mathbf{U}_1^H)\mathbf{Y}^H = \mathbf{T}_1\mathbf{\Sigma}_1^2\mathbf{S}_1 \tag{27}$$

Therefore, the two gramian product transpose relationships are

$$\mathbf{G}_c\mathbf{G}_o \approx \mathbf{T}_1\mathbf{\Sigma}_1^2\mathbf{S}_1, \qquad \mathbf{G}_o\mathbf{G}_c \approx \mathbf{S}_1^H\mathbf{\Sigma}_1^2\mathbf{T}_1^H \tag{28}$$

Equations (28) imply Eqs. (12) after employing the constraint relationship $\mathbf{S}_1\mathbf{T}_1 = \mathbf{T}_1^H\mathbf{S}_1^H = \mathbf{I}$.

III. Error Analysis

The analytical error bound of the reduced-order model was established by Enns [13] in the frequency domain:

$$\|G(i\omega) - G_r(i\omega)\|_\infty \le 2\left(\sum_{k=r+1}^{N}\sigma_k\right) \tag{29}$$

where σ_k is the kth HSV. For the single-input/single-output system the infinity norm is equal to the absolute value. This bound represents the best a reduced-order model can achieve using the approach of balanced truncation.

In this section we show that the empirical error bound based on a time-domain snapshot approach can be derived. The result is consistent with Eq. (29). We start by describing a rectangular data block $\mathbf{X}$ that has N rows and N_s columns ($N > N_s$). We form the empirical controllability gramian $\mathbf{W}_c = \mathbf{X}\mathbf{X}^H$, which is a Hermitian outer product. Even though the outer product is used in the paper, it is informative to know that we can also form a smaller-sized $N_s \times N_s$ Hermitian inner product with $\mathbf{X}$, $\hat{\mathbf{W}}_c = \mathbf{X}^H\mathbf{X}$. It can be shown that the first N_s eigenvalues of $\mathbf{W}_c$ are the same as the N_s eigenvalues of $\hat{\mathbf{W}}_c$. If we let $\mathbf{Q}_{c1}$ be the first N_s nonnormalized eigenvectors of $\mathbf{W}_c$ and let $\hat{\mathbf{U}}_{c1}$ be the N_s normalized eigenvectors of $\hat{\mathbf{W}}_c$, then we have $\mathbf{Q}_{c1} = \mathbf{X}\hat{\mathbf{U}}_{c1}$ [3,10].

A. Least-Squares-Error Technique

Consider a data block (order $N \times N_s$) in the form of the matrix $\mathbf{X} = [\mathbf{x}_1, \ldots, \mathbf{x}_{N_s}]$. Each of the N_s $N \times 1$ column vectors is a state vector, or snapshot, taken at t_k ($k = 1, 2, \ldots, N_s$). We have $\mathbf{x}_k = \mathbf{x}_c(t_k) = \exp(\mathbf{A}t_k)\mathbf{B}$. The quantity $\mathbf{X}\mathbf{X}^H$ is referred to as the

empirical controllability gramian, $\mathbf{W}_c$ (as opposed to the exact gramian $\mathbf{G}_c$). Typically, for large models we have $N_s < N$.

Let $\mathbf{X}$ be approximated by a preselected set of N_r basis vectors, represented by a $N \times N_r$ matrix $\mathbf{P}_1 = [\mathbf{p}_1, \ldots, \mathbf{p}_{N_r}]$. Typically, the number of snapshots sampled is greater than the number of reduced states, but much smaller than the number of original states, that is, we have $N_r < N_s \ll N$). In matrix notation, we write

$$\mathbf{X} = \mathbf{P}_1\mathbf{K} + \mathbf{E} \tag{30}$$

where the $N_r \times N_s$ weighting matrix $\mathbf{K}$ contains the coefficients to be determined. The $N \times N_s$ error matrix $\mathbf{E} = [\mathbf{e}_1, \ldots, \mathbf{e}_{N_s}]$ represents the total expansion error of $\mathbf{X}$; each column vector $\mathbf{e}_k$ is the state error vector of $\mathbf{x}_k$.

Since Eq. (30) is an overdetermined system ($N_s > N_r$) $\mathbf{K}$ can be determined by the well-known least-squares error (LSE) method, which minimizes the scalar functional $J = \mathrm{tr}(\mathbf{E}^H\mathbf{E})$, where $J = \|\mathbf{e}_1\|^2 + \cdots \|\mathbf{e}_{N_s}\|^2$. The LSE method gives

$$\mathbf{K} = \mathbf{P}_1^+\mathbf{X} \tag{31}$$

where $\mathbf{P}_1^+$ is defined as the Penrose pseudoinverse of $\mathbf{P}_1$, where $\mathbf{P}_1^+ = (\mathbf{P}_1^H\mathbf{P}_1)^{-1}\mathbf{P}_1^H$. Eliminating $\mathbf{K}$ in Eq. (30) by substitution, the error matrix $\mathbf{E}$ is then given by

$$\mathbf{E} = (\mathbf{I} - \mathbf{P}_1\mathbf{P}_1^+)\mathbf{X} \tag{32}$$

The error vectors, columns of $\mathbf{E}$, are orthogonal to the row vectors in the pseudoinverse; that is, $\mathbf{P}_1^+\mathbf{E} = \mathbf{0}$.

B. Karhunen–Loeve Expansion

The KL expansion is a special case of the LSE only with more benefits. In the KL expansion, the basis vectors of $\mathbf{P}_1$ are chosen to be the leading eigenvectors of $\mathbf{W}_c = \mathbf{X}\mathbf{X}^H$. This choice significantly improves the approximation, but at the expense of having to precompute these eigenvectors. The total error $\mathbf{E}$ is determined according to Eq. (32), with zero projection on $\mathbf{P}_1$. Unlike the LSE, the error structure of the truncated eigenvectors can be captured in the KL expansion by projecting on these vectors. Therefore, we need to consider a full-order set of basis vectors only for the error analysis. With SVD we have $\mathbf{W}_c = \mathbf{P}\mathbf{\Sigma}_c\mathbf{P}^H$, where $\mathbf{P}$ contains N orthonormal column eigenvectors. Note that the singular values of $\mathbf{\Sigma}_c$ are not the HSVs for the balanced gramians. Assuming that the ordered eigenvectors beyond the leading N_r are insignificant (as indicated by their singular values), we partition $\mathbf{P} = [\mathbf{P}_1\tilde{\mathbf{P}}]$, where $\mathbf{P}_1$ consists of basis vectors for the expansion, but the residual $\tilde{\mathbf{P}}$ consists of $N - N_r$ truncated eigenvectors whose errors associated with the expansion can be sized in an error analysis. Similarly, we partition $\mathbf{\Sigma}_c$ into diagonal blocks $\mathbf{\Sigma}_{c1}$ and $\tilde{\mathbf{\Sigma}}_c$.

In analogy to Eqs. (30) and (31), the KL expansion is governed by

$$\mathbf{X} = \mathbf{P}_1\mathbf{X}_r + \mathbf{E}, \qquad \mathbf{X}_r = \mathbf{P}_1^H\mathbf{X} \tag{33}$$

We have changed the notation $\mathbf{K}$ to $\mathbf{X}_r$ in anticipation of model reduction, the columns of $\mathbf{K}$ can then be considered as reduced-state vectors. Like Eq. (32), in the KL expansion we have

$$\mathbf{E} = (\mathbf{I} - \mathbf{P}_1\mathbf{P}_1^H)\mathbf{X} \tag{34}$$

The operators on the right-hand side of Eqs. (32) and (34) in the parentheses are projectors.

Since $\mathbf{P}_1^H\mathbf{P}_1 = \mathbf{I}$, from Eq. (34) we have $\mathbf{P}_1^H\mathbf{E} = \mathbf{0}$. Projection of $\mathbf{E}$ on $\tilde{\mathbf{P}}$ gives $\tilde{\mathbf{P}}^H\mathbf{E} = \tilde{\mathbf{P}}^H\mathbf{X}$. Using the relationship $\mathbf{P}^H\mathbf{W}_c\mathbf{P} = \mathbf{P}^H\mathbf{X}\mathbf{X}^H\mathbf{P} = \mathbf{\Sigma}_c$, we have the important result that $(\tilde{\mathbf{P}}^H\mathbf{E})(\tilde{\mathbf{P}}^H\mathbf{E})^H = \tilde{\mathbf{\Sigma}}_c$. For a simpler interpretation we seek projection of the error matrix $\mathbf{E}$ on individual orthonormal eigenvector $\mathbf{p}_k$, where $\mathbf{P} = [\mathbf{p}_1, \mathbf{p}_2, \ldots, \mathbf{p}_N]$. Accordingly, we have $\mathbf{p}_k^H\mathbf{E} = \mathbf{0}$ for $k = 1, \ldots, N_r$, and $\mathbf{p}_k^H\mathbf{E} = \mathbf{p}_k^H\mathbf{X}$ for $k = N_r + 1, \ldots, N_s$. Now we define the error vectors as basis-vector-based. The $\mathbf{p}_k$-based error vector is a $1 \times N_s$ row vector, $\boldsymbol{\epsilon}_k$, where we have $\boldsymbol{\epsilon}_k = \mathbf{p}_k^H\mathbf{E} = [\mathbf{p}_k^H\mathbf{e}_1, \ldots, \mathbf{p}_k^H\mathbf{e}_{N_s}]$. The components of the kth $\mathbf{p}_k$-based error vector consists of inner products of all state error vectors $\mathbf{e}_\ell$ on $\mathbf{p}_k$ ($\ell = 1, 2, \ldots, N_s$). Since $\mathbf{X}$ has $N_s < N$ columns, the last $N - N_s$ singular values are identically zero, i.e., $\sigma_{ck} = 0$ for $k = N_s + 1, \ldots, N$ (σ_{ck} is the kth entry of $\mathbf{\Sigma}_c$). Since $\mathbf{p}_k$ is an eigenvector of $\mathbf{X}\mathbf{X}^H$, we have $(\mathbf{X}\mathbf{X}^H)\mathbf{p}_k = \mathbf{p}_k\sigma_{ck}$. We have

$$\boldsymbol{\epsilon}_k\boldsymbol{\epsilon}_\ell^H = (\mathbf{p}_k^H\mathbf{E})(\mathbf{p}_\ell^H\mathbf{E})^H = \mathbf{p}_k^H\mathbf{X}\mathbf{X}^H\mathbf{p}_\ell = \sigma_{c\ell}\delta_{k\ell}, \quad k, \ell = N_r + 1, \ldots, N \tag{35}$$

because of $\mathbf{p}_k^H\mathbf{p}_\ell = \delta_{k\ell}$.

We conclude that 1) the set of all error vectors, $\boldsymbol{\epsilon}_k$, is mutually orthogonal; 2) the square of the magnitude of each error vector is equal to the corresponding singular value. In summary, we have the following result:

$$\|\boldsymbol{\epsilon}_k\|^2 = \begin{cases} 0, & \text{for } k = 1, 2, \ldots, N_r \\ \sigma_{ck}, & \text{for } k = N_r + 1, \ldots, N_s \\ 0, & \text{for } k = N_s + 1, \ldots, N \end{cases} \tag{36}$$

There is no quantitative estimate for residual errors in LSE as in the KL expansion. LSE relies on an increasing number of basis vectors to reduce the total error. In the KL expansion, by picking specific basis vectors one obtains a quantitative measure of the error residual. In the KL expansion, the left projection is done by the conjugate/transpose of $\mathbf{P}_1$. Whether the full-order state-space system generating the data block $\mathbf{X}$ is normal or nonnormal, the KL expansion error analysis is valid.

C. Generalized KL Expansions

For the model reduction of nonnormal systems, the controllability data block $\mathbf{X}$ can be used to extract the set of basis vectors for column reduction of the state-space model. The observability data block $\mathbf{Y}$ can be used to extract the set of basis vectors for row reduction of the state-space model. The data block $\mathbf{X}$ is generated from $\mathbf{x}_c(t_i) = \exp(\mathbf{A}t_i)\mathbf{B}$, for sampling times t_i ($i = 1, 2, \ldots, N_s$); $\mathbf{Y}$ is generated by the adjoint state vectors $\mathbf{x}_o(t_j) = \exp(\mathbf{A}^H t_j)\mathbf{C}^H$, for sampling times t_j ($j = 1, 2, \ldots, N_s$). As we see in Eqs. (50), balancing of the two sets of basis vectors give RBT.

The generalized KL expansion deals with two data blocks, one generated from controllability snapshots and the other from observability snapshots. The dual-state basis functions are provided from the RBT. The dual-block expansion residual errors can be determined analytically. To analyze the residual errors of the expansions, it is necessary to consider the complete sets of basis vectors in $\mathbf{S}$ and $\mathbf{T}$. The partition of the balancing transformations is shown in Eqs. (9). The partition of the constraint condition is given by Eqs. (11). Unlike in the KL expansion, there is no orthogonality relationship in the basis vectors other than that specified in Eqs. (11).

Using the RBT in the generalized KL expansion, Eq. (33) of the KL expansion can be extended to the following two expansions:

$$\begin{aligned} \mathbf{X} &= \mathbf{T}_1\mathbf{X}_r + \mathbf{E}_c, \qquad \mathbf{X}_r = \mathbf{S}_1\mathbf{X} \\ \mathbf{Y} &= \mathbf{S}_1^H\mathbf{Y}_r + \mathbf{E}_o, \qquad \mathbf{Y}_r = \mathbf{T}_1^H\mathbf{Y} \end{aligned} \tag{37}$$

where $\mathbf{X}_r$ and $\mathbf{Y}_r$ are the coefficient matrices. The RBT $\mathbf{S}_1$ and $\mathbf{T}_1$ are given by Eqs. (26), or in the alternative form, by Eqs. (20). The residual matrix $\mathbf{E}_c$ ($N \times N_s$) in the expansion represents the total error of $\mathbf{X}$, and the residual matrix $\mathbf{E}_o$ ($N \times N_s$) in the expansion represents the total error of $\mathbf{Y}$.

For error analysis the total errors in the generalized KL expansion can be expressed as

$$\mathbf{E}_c = (\mathbf{I} - \mathbf{T}_1\mathbf{S}_1)\mathbf{X}, \qquad \mathbf{E}_o = (\mathbf{I} - \mathbf{S}_1^H\mathbf{T}_1^H)\mathbf{Y} \tag{38}$$

The operators defined in the parenthesis on the right-hand side of the equations are projectors. Let $\mathbf{s}_i$ be the row vectors of $\mathbf{S}$, and let $\mathbf{t}_j$ be the column vectors of $\mathbf{T}$ ($i, j = 1, 2, \ldots, N$). From Eq. (5), by replacing $\mathbf{G}_c$ by $\mathbf{X}\mathbf{X}^H$ and $\mathbf{G}_o$ by $\mathbf{Y}\mathbf{Y}^H$, we have

$$(\mathbf{X}\mathbf{X}^H)\mathbf{s}_k^H = \mathbf{t}_k\sigma_k, \qquad (\mathbf{Y}\mathbf{Y}^H)\mathbf{t}_k = \mathbf{s}_k^H\sigma_k, \qquad k = 1, 2, \ldots, N \tag{39}$$

where σ_k ($k = 1, \ldots, N$) are the HSVs. Note that the RBT consists of $(\mathbf{s}_k, \mathbf{t}_k)$, for $k = 1, 2, \ldots, N_r$. The residual vectors $(\tilde{\mathbf{S}}, \tilde{\mathbf{T}})$ consist of $(\mathbf{s}_k, \mathbf{t}_k)$, for $k = N_r + 1, \ldots, N_s$. The last $N - N_s$ eigenvector pairs are irrelevant because their σ_k are identically zero.

Taking the inner products of the first equation of Eqs. (38) by $\mathbf{S}_1$ and the second equation by $\mathbf{T}_1^H$, we obtain $\mathbf{S}_1\mathbf{E}_c = \mathbf{0}$ and $\mathbf{T}_1^H\mathbf{E}_o = \mathbf{0}$, respectively. Similarly, taking the inner products by the tilde eigenvector sets gives $\tilde{\mathbf{S}}\mathbf{E}_c = \tilde{\mathbf{S}}\mathbf{X}$ and $\tilde{\mathbf{T}}^H\mathbf{E}_o = \tilde{\mathbf{T}}^H\mathbf{Y}$. In the product form, we have $(\tilde{\mathbf{S}}\mathbf{E}_c)(\mathbf{E}_c^H\tilde{\mathbf{S}}^H) = \tilde{\mathbf{S}}\mathbf{X}\mathbf{X}^H\tilde{\mathbf{S}}^H$ and $(\tilde{\mathbf{T}}^H\mathbf{E}_o)(\mathbf{E}_o^H\tilde{\mathbf{T}}) = \tilde{\mathbf{T}}^H\mathbf{Y}\mathbf{Y}^H\tilde{\mathbf{T}}$. Substituting $\mathbf{X}\mathbf{X}^H$ and $\mathbf{Y}\mathbf{Y}^H$ using Eqs. (39), we obtain

$$(\mathbf{s}_k\mathbf{E}_c)(\mathbf{s}_\ell\mathbf{E}_c)^H = \sigma_\ell\delta_{k\ell}, \qquad (\mathbf{t}_k^H\mathbf{E}_o)(\mathbf{t}_\ell^H\mathbf{E}_o)^H = \sigma_\ell\delta_{k\ell}$$
$$k, \ell = N_r + 1, \ldots, N \tag{40}$$

We define the $1 \times N_s$ basis-vector-based error vectors for $\mathbf{X}$ and $\mathbf{Y}$ by $\boldsymbol{\epsilon}_{ck} = \mathbf{s}_k\mathbf{E}_c$ and $\boldsymbol{\epsilon}_{ok} = \mathbf{t}_k^H\mathbf{E}_o$, respectively, then we have

$$\|\boldsymbol{\epsilon}_{ck}\|^2 = \begin{cases} 0, & \text{for } k = 1, 2, \ldots, N_r \\ \sigma_k, & \text{for } k = N_r + 1, \ldots, N_s \\ 0, & \text{for } k = N_s + 1, \ldots, N \end{cases} \tag{41}$$

and

$$\|\boldsymbol{\epsilon}_{ok}\|^2 = \begin{cases} 0, & \text{for } k = 1, 2, \ldots, N_r \\ \sigma_k, & \text{for } k = N_r + 1, \ldots, N_s \\ 0, & \text{for } k = N_s + 1, \ldots, N \end{cases} \tag{42}$$

According to the above expansions, a column vector in $\mathbf{X}$ and one in $\mathbf{Y}$ at given times t_i and t_j, respectively, can be expressed as $\exp(\mathbf{A}t_i)\mathbf{B} = \mathbf{T}_1\mathbf{X}_r(t_i)$ and $\exp(\mathbf{A}^H t_j)\mathbf{C}^H = \mathbf{S}_1^H\mathbf{Y}_r(t_j)$, respectively. At time zero, one can write $\mathbf{B} = \mathbf{T}_1\mathbf{B}_r$ and $\mathbf{C}^H = \mathbf{S}_1^H\mathbf{C}_r^H$. The inverse relationships for the reduced column vectors are

$$\mathbf{X}_r(t_i) = \mathbf{S}_1\exp(\mathbf{A}t_i)\mathbf{T}_1\mathbf{B}_r, \qquad \mathbf{Y}_r^H(t_j) = \mathbf{C}_r\mathbf{S}_1\exp(\mathbf{A}t_j)\mathbf{T}_1 \tag{43}$$

To qualitatively relate Eq. (29) to the present time-domain error analysis, we note that the full-order input-to-output quantity $\mathbf{C}\exp(\mathbf{A}t)\mathbf{B}$ is the inverse Laplace transform of $G(s)$. The reduced-order quantity can be formed from Eq. (43), $\mathbf{C}_r\mathbf{S}_1\exp(\mathbf{A}t)\mathbf{T}_1\mathbf{B}_r$. It can be shown (albeit involving some lengthy algebraic manipulations), that this quantity has the same order of error as $\mathbf{C}_r\exp(\mathbf{S}_1\mathbf{A}\mathbf{T}_1 t)\mathbf{B}_r$, which is the inverse Laplace transform of $G_r(s)$.

D. ROM Errors: BPOD, POD, Modified POD, and PBPOD

In the KL expansion, a single data block $\mathbf{X}$ is approximated by a basis-vector matrix $\mathbf{U}_{c1}$ consists of leading eigenvectors of the outer-product quantity $\mathbf{W}_c = \mathbf{X}\mathbf{X}^H$, and the coefficients of the expansion are determined by projecting the data block on the conjugate/transpose of the matrix. The error analysis shows that the expansion errors are bounded. So in the well-known POD method, the following reduced transformation is used to obtain the ROM:

$$\mathbf{S}_{1p} = \mathbf{U}_{c1}^H, \qquad \mathbf{T}_{1p} = \mathbf{U}_{c1} \tag{44}$$

Note that $\mathbf{S}_{1p}\mathbf{T}_{1p} = \mathbf{I}$ because the eigenvectors in $\mathbf{U}_{c1}$ are orthonormal. Equation (44) can approximate a single data block $\mathbf{X}$ very well, but it cannot simultaneously approximate $\mathbf{X}$ and the adjoint block $\mathbf{Y}$ well, unless both blocks are generated by a normal system. If the system is nonnormal, Eq. (44) will produce a ROM that is inaccurate.

For a good approximation of the ROM of a nonnormal system, without performing balancing (like in the RBT of Sec. II.B.2), we have to consider leading eigenvectors from both data blocks, $\mathbf{W}_c = \mathbf{X}\mathbf{X}^H$ and $\mathbf{W}_o = \mathbf{Y}\mathbf{Y}^H$. For error analysis we apply the KL expansion twice, one for each gramian. We keep only the dominant eigenvector sets and denote $\mathbf{W}_c \approx \mathbf{U}_{c1}\boldsymbol{\Sigma}_{c1}\mathbf{U}_{c1}^H$ and $\mathbf{W}_o \approx \mathbf{U}_{o1}\boldsymbol{\Sigma}_{o1}\mathbf{U}_{o1}^H$ (both eigenvector matrices are $N \times N_r$), where $\mathbf{U}_{o1}$ are the leading eigenvectors of $\mathbf{W}_o = \mathbf{Y}\mathbf{Y}^H$. For a nonnormal input/output system, its ROM has the form

$$(\mathbf{U}_{o1}^H\mathbf{U}_{c1})\dot{\mathbf{x}}_r = (\mathbf{U}_{o1}^H\mathbf{A}\mathbf{U}_{c1})\mathbf{x}_r + (\mathbf{U}_{o1}^H\mathbf{B})u, \qquad y = (\mathbf{C}\mathbf{U}_{c1})\mathbf{x}_r \tag{45}$$

Therefore, the nonbalanced, reduced transformation for the modified POD is given by

$$\mathbf{S}_{1mp} = (\mathbf{U}_{o1}^H\mathbf{U}_{c1})^{-1}\mathbf{U}_{o1}^H, \qquad \mathbf{T}_{1mp} = \mathbf{U}_{c1} \tag{46}$$

The inverse matrix factor in the first equation is for normalization so that $\mathbf{S}_{1mp}\mathbf{T}_{1mp} = \mathbf{I}$. Since $\mathbf{U}_{c1}$ consists of leading eigenvectors of the controllability gramian and $\mathbf{U}_{o1}$ consists of leading eigenvectors of the observability gramian, the KL expansion should be applicable twice separately without major changes. This is a nonbalanced dual-state approach to obtain a reduced transformation. Unlike POD, the method of modified POD appears to be effective for nonnormal systems. However, since the algorithms for obtaining RBT are quite simple, not much is gained by switching to the modified POD approach.

Of particular interest is whether a matrix factor $\boldsymbol{\Phi}$ can be incorporated into Eq. (46) such that the nonbalanced transformation can be converted to a variant form of RBT. The RBT can be expressed as

$$\mathbf{S}_1 = (\mathbf{U}_{o1}^H\mathbf{U}_{c1}\boldsymbol{\Phi})^{-1}\mathbf{U}_{o1}^H, \qquad \mathbf{T}_1 = \mathbf{U}_{c1}\boldsymbol{\Phi} \tag{47}$$

where $\boldsymbol{\Phi}$ is a $N_r \times N_r$ matrix that cannot violate the constraint $\mathbf{S}_1\mathbf{T}_1 = \mathbf{I}$.

One way to obtain $\boldsymbol{\Phi}$ is to compare the above transformation equation (47) with the RBT based on the SVD method (Sec. II.B.2). From the SVD of the empirical gramians above, we define a a $N_r \times N_r$ generalized Hankel matrix $\mathbf{H}_{mp} = \boldsymbol{\Sigma}_{o1}^{1/2}\mathbf{U}_{o1}^H\mathbf{U}_{c1}\boldsymbol{\Sigma}_{c1}^{1/2}$. This $\mathbf{H}_{mp}$ resembles the product $\mathbf{Y}^H\mathbf{X}$ defined in Sec. II.B.2. Applying SVD we have $\mathbf{H}_{mp} = \mathbf{U}_{mp}\boldsymbol{\Sigma}_{mp}\mathbf{V}_{mp}^H$, where all the matrices with subscript mp are square. Thus, we have

$$\boldsymbol{\Sigma}_{o1}^{1/2}\mathbf{U}_{o1}^H\mathbf{U}_{c1}\boldsymbol{\Sigma}_{c1}^{1/2} = \mathbf{U}_{mp}\boldsymbol{\Sigma}_{mp}\mathbf{V}_{mp}^H \tag{48}$$

The above equation can be further expressed as

$$(\boldsymbol{\Sigma}_{mp}^{-1/2}\mathbf{U}_{mp}^H\boldsymbol{\Sigma}_{o1}^{1/2}\mathbf{U}_{o1}^H)(\mathbf{U}_{c1}\boldsymbol{\Sigma}_{c1}^{1/2}\mathbf{V}_{mp}\boldsymbol{\Sigma}_{mp}^{-1/2}) = \mathbf{I} \tag{49}$$

We define the above relationship as $\mathbf{S}_1\mathbf{T}_1 = \mathbf{I}$. Thus, we let

$$\mathbf{S}_1 = (\boldsymbol{\Sigma}_{mp}^{-1/2}\mathbf{U}_{mp}^H\boldsymbol{\Sigma}_{o1}^{1/2})\mathbf{U}_{o1}^H, \qquad \mathbf{T}_1 = \mathbf{U}_{c1}(\boldsymbol{\Sigma}_{c1}^{1/2}\mathbf{V}_{mp}\boldsymbol{\Sigma}_{mp}^{-1/2}) \tag{50}$$

Comparing Eq. (50) with Eq. (47), we let

$$\boldsymbol{\Phi} = \boldsymbol{\Sigma}_{c1}^{1/2}\mathbf{V}_{mp}\boldsymbol{\Sigma}_{mp}^{-1/2} \tag{51}$$

Then we need to further show that the following holds:

$$(\mathbf{U}_{o1}^H\mathbf{U}_{c1}\boldsymbol{\Phi})^{-1} = \boldsymbol{\Sigma}_{mp}^{-1/2}\mathbf{U}_{mp}^H\boldsymbol{\Sigma}_{o1}^{1/2} \tag{52}$$

One way to show that Eq. (52) holds without getting into too much complicated algebraic manipulations is by substituting the expression of $\boldsymbol{\Phi}$ into the left-hand side, then inverting the left-hand term to the right of the right-hand side of the equation. Then we recover Eq. (49). The modified POD method is not significantly simpler than the BPOD using the RBT.

The PBPOD [2,3] was considered in our previous studies mainly motivated by nonlinear model reduction, which does not possess the kind of duality that linear model-reduction uses. The word "pseudobalanced" comes from the fact that PBPOD simultaneously diagonalizes the gramians, but only in the retained block. Ma et al. [14] pointed out the deficiency of PBPOD in that the cross-diagonal blocks, unlike BPOD, incur nonzero entries. In fact, the pseudobalanced ROM generated by PBPOD appears more akin to

the ROM generated from POD. The reduced transformation of PBPOD is

$$\mathbf{S}_{1pp} = \mathbf{T}_1^+, \qquad \mathbf{T}_{1pp} = \mathbf{T}_1 \tag{53}$$

where $\mathbf{T}_{1pp}$ is the same $\mathbf{T}_1$ derived in BPOD, whereas $\mathbf{S}_{1pp}$ is not derived from the observability data like in BPOD, but from the pseudoinverse of $\mathbf{T}_1$.

IV. Results

The Orr–Sommerfeld system with wall input/output provides a good example of a nonnormal time-invariant state-space system. To reduce the size of this paper, we refer readers to [2–4] for the derivations and physical description. The system depends on two prescribed parameters: the Reynolds number Re and wave number k.

Nonnormality is an important motivation of this study. It is worthwhile to provide a simple illustration of a second-order example, like we did in Or et al. [4]. This example was first communicated to us by Rowley [10]. Consider

$$\mathbf{A} = \begin{bmatrix} -1 & 10 \\ 0 & -5 \end{bmatrix}$$

$$\mathbf{B} = \begin{bmatrix} 1 \\ 1 \end{bmatrix}$$

$$\mathbf{C} = [1 \quad 1]$$

$D = 0$. Although the input and output vectors are identical, $\mathbf{A}$ is clearly nonsymmetric, but with negative eigenvalues (likewise, nonnormality can also be demonstrated by constructing a symmetric $\mathbf{A}$, but asymmetric input and output vectors). In the baseline, the gramians are

$$\mathbf{G}_c = \begin{bmatrix} 3.83 & 0.33 \\ 0.33 & 0.1 \end{bmatrix}$$

$$\mathbf{G}_o = \begin{bmatrix} 0.5 & 1 \\ 1 & 2.1 \end{bmatrix}$$

Upon balancing the diagonal gramian is

$$\mathbf{\Sigma} = \begin{bmatrix} 1.67 & 0 \\ 0 & 0.07 \end{bmatrix}$$

The two HSVs are dominated by the first, which justifies a truncation to a first-order system. Indeed, taking SVD of the gramians shows that each gramian only has one dominant SV. In the baseline RBT, we determine $\mathbf{S}_1 = [-0.81 \; -1.64]$ and

$$\mathbf{T}_1 = \begin{bmatrix} -0.99 \\ -0.12 \end{bmatrix}$$

In POD, the first eigenvector of $\mathbf{G}_c$ is

$$\mathbf{U}_{c1} = \begin{bmatrix} -0.10 \\ -0.09 \end{bmatrix}$$

For the baseline balanced ROM we obtain $\mathbf{S}_1\mathbf{A}\mathbf{T}_1 = -0.82$, $\mathbf{S}_1\mathbf{B} = -2.45$, and $\mathbf{C}\mathbf{T}_1 = -1.11$, and for POD we obtain $\mathbf{U}_{c1}^H\mathbf{A}\mathbf{U}_{c1} = -0.15$, $\mathbf{U}_{c1}^H\mathbf{B} = -1.08$, and $\mathbf{C}\mathbf{U}_{c1} = -1.08$. Figure 1 shows the output response $y(t)$ of a unit step. Clearly, the balanced ROM output agrees with the original model output, but the POD ROM output does not.

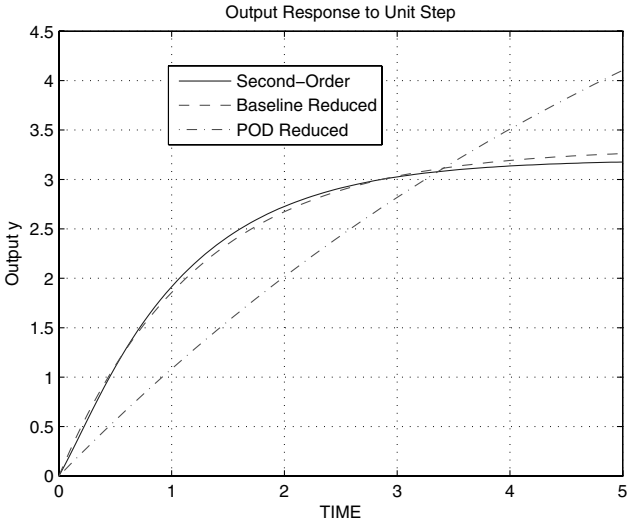

Fig. 1 Compare an output response to a unit step using a second-order model and its ROMs.

In the following, key comparisons in terms of open-loop responses to a unit input of the Orr–Sommerfeld system for sufficiently long duration are given. Error norms are plotted to validate the theory of the generalized KL expansion.

A. Comparison of the Balanced ROMs Constructed by RBTs from Different Methods

First, we compare the output responses of a unit step input, simulated by balanced ROMs constructed from RBTs obtained using different methods, but all based on the exact solution of the gramians. These methods include the baseline (Sec. II.A), the eigenvector method (Sec. II.B.1) and the SVD method (Sec. II.B.2), as previously discussed. We consider a stable region where $Re = 5000$ and $k = 1$. The original model has $N = 128$. As initial conditions, we set $\mathbf{x} = \mathbf{0}$ for the original model and $\mathbf{x}_r = \mathbf{0}$ for the ROMs. The length of simulation should be long enough to capture the essential performance characteristics. We use an Euler scheme with an integration time step of magnitude 0.001. The responses shown cover 60 thousand time steps. An implicit-Euler scheme allows bigger time step for numerical stability, but gives the same result. The interval between successive sampled outputs is 100 steps. The baseline version of RBT is obtained by the balanced truncation. In Fig. 2, all the three balanced ROMs have $N_r = 10$. The left-side panels show

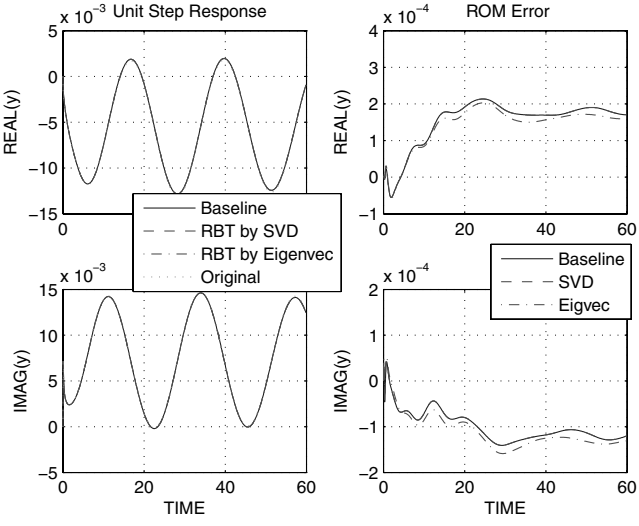

Fig. 2 Comparison of the output responses of the ROMs projected by RBTs computed using exact gramians.

the real part (upper) and imaginary part (lower) of the output response to a unit step input. The baseline ROM (solid line), the ROM constructed by the SVD-based RBT (dashed line), the ROM constructed by the eigenvector-based RBT (dash-dotted line), and the full-order original model (dotted line) are all captured in the figures. Their response curves collapse visually almost into a single curve. The agreement is very good for the simulation duration. From the result we conclude that all three methods for generating RBTs are in agreement. The right-side panels show the response errors of the ROMs. The error is the output difference between the ROM and the original model. The errors are more than an order of magnitude smaller than the output, further suggesting that the ROMs consisting of 10 balanced modes ($N_r = 10$) are adequate.

In the second case we compare the same output responses of the ROMs, but now the empirical gramians are used to generate the RBTs. All parameters remain unchanged from the first case, including the time step for numerical integration. Again, the output of the ROM constructed by the baseline RBT is compared with the ROMs constructed with the RBTs using the eigenvector-based method and the SVD-based method. However, in computing the empirical gramians, the sampling of the controllability and observability data blocks employs a two-sample time snapshot technique that is the same as described in our previous paper [3] to preserve some continuity and because the two-sample technique show good performance. In the snapshot scheme, we use an implicit-Euler scheme with a larger time step of 0.01 (a similar result is achieved by using the explicit Euler scheme with smaller time step of 0.0001). Two sampled intervals are used. The first generates 60 state vectors (and adjoint state vectors) at a three-time-step sampled interval, followed by the second with 60 state vectors (and adjoint state vector) at a 30-time-step sampled interval. At the time of the study [3] the parameters chosen for this snapshot sampling scheme were quite well-justified. However, one can still argue that there is room for improvement in the empirical gramians.

The results are shown in Fig. 3. The baseline response curve (solid line) and the original model response curve (dotted line) remain the same as in Fig. 2. However, we observe that the SVD-based ROM output response curve (dashed line) and the eigenvector-based ROM output response curve (dash-dotted line) show larger deviation than their counterpart of Fig. 2. The corresponding response error curves are shown on the right-side panels. We conclude that the significant larger response errors are due to the approximation errors of the empirical gramians. Since both sets of results are based on $N_r = 10$ only, it should be noted that better performance can be achieved for the same gramians by increasing N_r in the RBT. The empirical data blocks $\mathbf{X}$ and $\mathbf{Y}$, in which each contains 120 snapshots, are comparable in size with N.

Comparing the results in Figs. 2 and 3 suggests that greater errors are induced by the empirical approximation of the gramians than by state truncation. Therefore, the results highlight room for improvement in the snapshot approach. Of course, the performance of the balanced ROMs can always be improved by increasing the order of the model, N_r.

B. Comparison of ROM Responses from BPOD, POD, and PBPOD

For this example it is of interest is to see how the performances of the PBPOD and POD compared with the BPOD. Their reduced transformations are described in Sec. III.D. Figure 4 shows the output response to a unit input, generated from the ROMs based on the PBPOD method (dash-dotted lines) and the POD method (dotted lines). In this case we use $N_r = 28$ for BPOD, PBPOD, and POD. With more than double the number of modes included, we see that the BPOD curve (dashed lines) now agrees very well with the original model (solid lines), even though the same empirical gramians as in Fig. 3 are used. The BPOD performance in Fig. 4 clearly improves over that in Fig. 3. We observe that the imaginary part of the output response curves of PBPOD and POD show a bias offset, though the real part agrees with that from BPOD for the first half of the period. For the second half of the period, the deviations are significantly larger. The drawback of PBPOD for the nonnormal system is not as obvious by comparing the gain/phase frequency plots shown in our previous study [3].

We conclude this comparison section by showing in Fig. 5 how the ROM output errors of the modified POD methods compared with the baseline ROM error (refer to Fig. 2, panels on the right-hand side). There are two cases for the modified POD, one with the factor $\mathbf{\Phi}$ to balance the reduced transformation and the other case does not have the factor and is nonbalanced. Like in the first case, we subtract the full-order model output response from the reduced-order model output response to generate the error curve. In the results, the real part of the errors is shown on the left panel and the imaginary part is shown on the right panel. Again, $N_r = 10$ is used. The baseline error curves are identical to those of Fig. 2. Surprisingly, the errors from the modified POD are on the order of 10^2 smaller than those of the baseline. The errors of the modified POD are a lot more rapidly oscillatory than those of the baseline. An important observation is that in the OS system under study, the singular-value (SV) magnitudes between the two gramians differ significantly. The SVs are shown later in Figs. 6 and 7. We would expect that the balanced-and-truncated is more accurate than the case of truncated-and-then-balanced done here. But the result here of using a low truncation number $N_r = 10$ for both gramian eigenvectors suggests that balancing actually does not significantly improve accuracy. Even without the balancing factor involved, the modified POD seems more

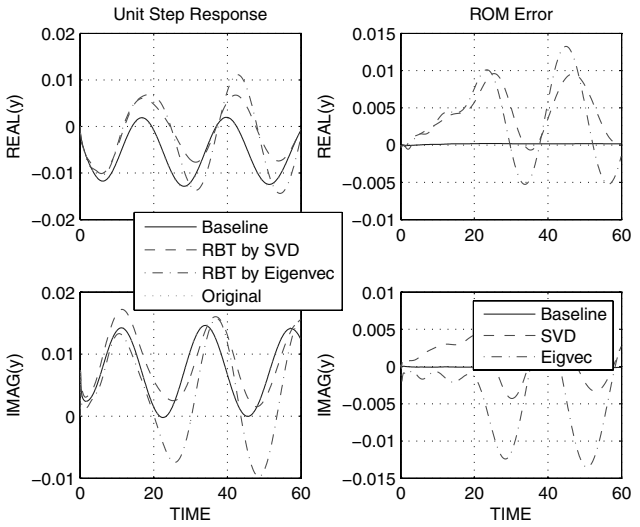

Fig. 3 Comparison of the output responses of the ROMs projected by RBTs computed using empirical gramians.

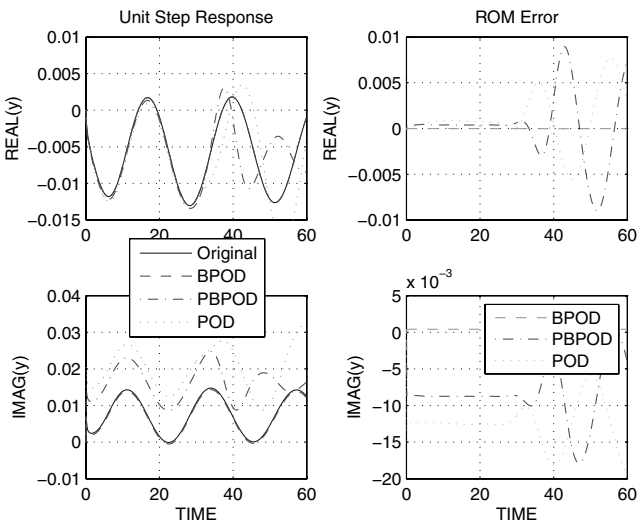

Fig. 4 Comparison of the output responses of the ROMs generated by PBPOD, POD, and BPOD.

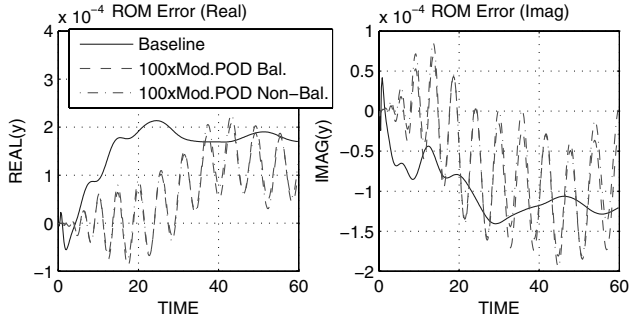

Fig. 5 Comparison of the output errors of the baseline balanced ROM, the ROM of modified POD (balanced) and the ROM of modified POD (nonbalanced).

accurate that BPOD for this particular case. The significance of the modified POD is clear from a theoretical point of view. First, a dual-state approach is essential for the model reduction of a nonnormal system. Second, once a dual-state approach is in place, performing balancing (or not) may be a less critical step.

C. Error Bounds of the Generalized KL Expansion

The error bound of KL expansion is well known [9]. Our numerical results verify that Eqs. (36) hold for a single data block. Therefore, we mainly focus on the generalized KL expansion. We first consider data blocks generated from the exact solution of gramians and then data blocks generated from the empirical gramians. Comparing these two cases will show performance of the snapshot approach. In the exact-solution approach, the two data blocks are denoted by $\mathbf{X}$ and $\mathbf{Y}$ (with $N_s = N$), where we have $\mathbf{X}\mathbf{X}^H = \mathbf{G}_c$ and $\mathbf{Y}\mathbf{Y}^H = \mathbf{G}_o$. The columns of the data blocks are the orthonormal eigenvectors of the gramians, scaled by the square root of the respective singular values. The generalized KL expansion is given by Eqs. (37), where the reduced transformation $(\mathbf{S}_1, \mathbf{T}_1)$ is used in the expansion corresponds to the RBT, with $N_r = 10$. In Figs. 6a–6d, the same thin solid line represents the distribution of the HSVs. The HSVs are the reference points of the error bounds. Figures 6a–6c correspond to error projection and Fig. 6d shows the observability and controllability singular values and HSVs. In Fig. 6a, the square of the error vector norms, $\|\boldsymbol{\epsilon}_{ck}\|^2$ $(k = 1, 2, \ldots, N_s)$, generated by the inner products of the error vectors, $\boldsymbol{\epsilon}_{ck} = \mathbf{s}_k \mathbf{E}_c$, are shown in dots, Eq. (41). Likewise, the square of the error vector norms, $\|\boldsymbol{\epsilon}_{ok}\|^2$ $(k = 1, 2, \ldots, N_s)$ by the inner products of the error vectors $\boldsymbol{\epsilon}_{ok} = \mathbf{t}_k^H \mathbf{E}_o$, are shown in crosses, Eq. (42). The square of error

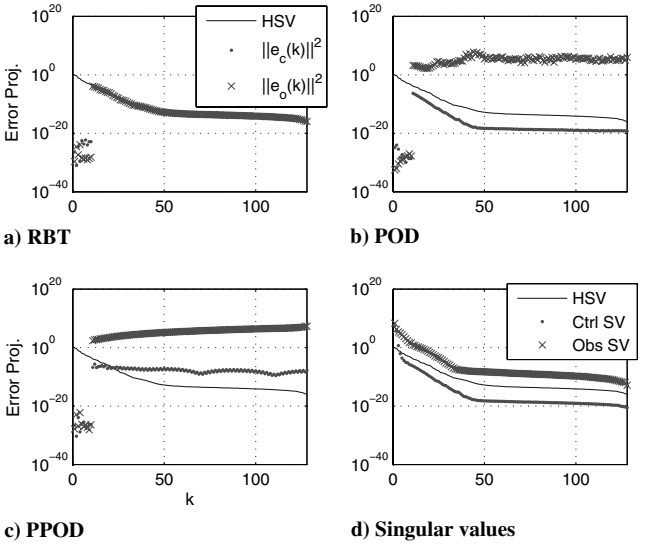

Fig. 6 Error bounds in the generalized KL expansion based on exact solutions of gramians.

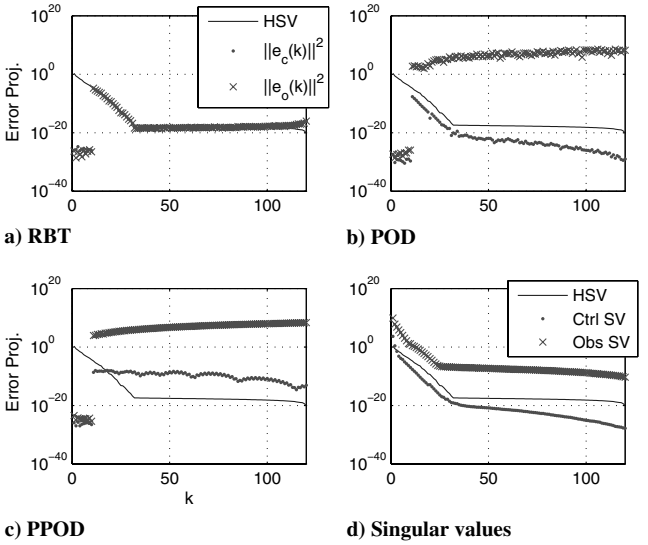

Fig. 7 Error bounds in the generalized KL expansion based on empirical gramians.

vector norms for the first $N_r = 10$ components are orders of magnitude smaller. The residual components, from the N_r^{th} to the $(N_r + 1)^{\text{th}}$ component, exhibits a discontinuous jump. After the jump, both residual components, $\|\boldsymbol{\epsilon}_{ck}\|^2$ and $\|\boldsymbol{\epsilon}_{ok}\|^2$, roll off but stay on the HSV curve, as predicted by the analytical results of Eqs. (41) and (42). If we keep more basis vectors by increasing N_r, the jump becomes less pronounced.

Next, we substitute other reduced transformations, such as POD [Eq. (44)] and PBPOD [Eq. (53)], respectively, for the RBT. We substitute $\mathbf{S}_1$ and $\mathbf{T}_1$ using the appropriate reduced transformation, and we apply the generalized KL expansion. The idea is to see how the error bounds shift. Figures 6b and 6c show the error points relative to the HSV curve.

In Figs. 6b and 6c, the first $N_r = 10$ error norms associated with $\mathbf{E}_c$ (dots) and $\mathbf{E}_o$ (crosses) are many orders of magnitude smaller than those of the HSVs. However, after the jump and from $k = N_r + 1$ to N_s, the two residual curves no longer track the HSV curve. This is a behavior unlike the RBT in Fig. 6a. The controllability error components associated with $\mathbf{E}_c$ (dots) are slightly below the HSV curve, so the errors are small. However, the observability error components (associated with $\mathbf{E}_o$) are large and above $\mathcal{O}(1)$ magnitude, way above the HSV curve. With the reduced transformation of PBPOD, Fig. 6c similar behavior as Fig. 6b. In Fig. 6d we plot the SVs of the controllability gramian (dots) and the observability gramian (crosses) against the HSVs. We conclude that for this OS system, the SVs of the observability gramian are roughly one to 2 orders of magnitude greater than the SVs of the controllability gramian. Using BPOD balancing converts both gramians to a diagonal form with the HSVs. In the nonbalanced approach, it appears that more observability basis vectors have to be retained than controllability basis vectors because the leading observability singular values are orders of magnitude larger than the leading controllability singular values.

We perform a similar error bound analysis using the empirical-based data blocks, $\mathbf{X}$ and $\mathbf{Y}$, to generate the gramians. Now $\mathbf{X}$ and $\mathbf{Y}$ are $N \times N_s$ matrices (where we use $N_s = 120 \neq N = 128$). Figures 7a–7d can be compared one to one with those panels of Fig. 6. In Fig. 7a, we observe that with the empirically generated data, the HSV curve roll off significantly more rapidly than the previous between $k = 1$ and 27. Then the HSV curve becomes practically flat, probably due to the limitation of numerical accuracy imposed on the snapshot data. Also, the tail portion shows minor deviations, which are probably of numerical nature. Again, Fig. 7a satisfies the analytical prediction of Eqs. (41) and (42). In Figs. 7b and 7c, with the reduced transformations of POD and PBPOD, we see similar characteristics as in Fig. 6. The SVs in Fig. 7d behave in a very similar fashion to those in Fig. 6d. We conclude that with good sampling

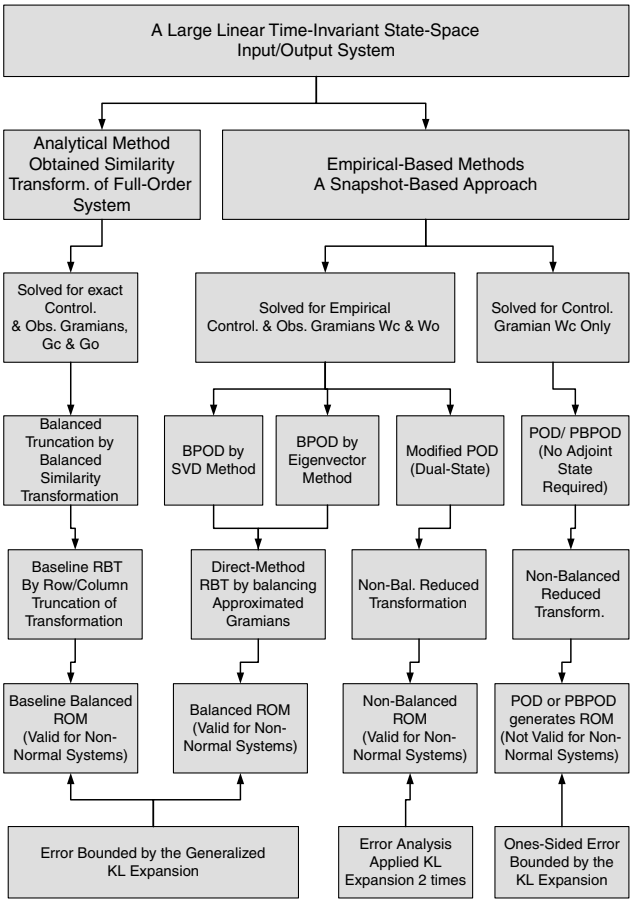

Fig. 8 Flow diagram of the various model-reduction methods for a large linear state-space model.

techniques, the snapshot approach appears to be effective at generating good approximation of the gramians.

V. Conclusions

In this study, several methods for model reduction applicable to large, nonnormal, linear time-invariant state-space systems are presented. A flow diagram is used to summarize these methods and their properties. All of the methods use some sort of reduced transformations for projecting the state-space matrices. Of particular emphasis are the reduced balanced transformation and the error analysis associated with it that generalizes the KL expansion to a dual-state application for nonnormal systems. Note that for nonlinear systems a state duality does not exist, and it is currently difficult to use snapshot methods for nonlinear input/output systems. This difficulty was the motivation for creating PBPOD from POD.

References

[1] Joshi, S. S., Speyer, J. L., and Kim, J., "Finite-Dimensional Optimal Control of Poiseuille Flow," *Journal of Guidance, Control, and Dynamics*, Vol. 22, 1999, pp. 340–348. doi:10.2514/2.4383

[2] Or, A. C., and Speyer, J. L. "Empirical Pseudo-Balanced Model Reduction and Feedback Control of Weakly Nonlinear Convection Patterns," *Journal of Fluid Mechanics*, Vol. 662, 2010, pp. 36–65. doi:10.1017/S0022112010002879

[3] Or, A. C., and Speyer, J. L., "Model reduction of Input-Output Dynamical Systems by Proper Orthogonal Decomposition," *Journal of Guidance, Control, and Dynamics*, Vol. 31, 2008, pp. 322–328. doi:10.2514/1.29456

[4] Or, A. C., Speyer, J. L., and Kim, J., "State-Space Approximations of the Orr–Sommerfeld System with Boundary Inputs and Outputs," *Journal of Guidance, Control, and Dynamics*, Vol. 33, 2010, pp. 794–802. doi:10.2514/1.46479

[5] Chen, C. T. *Linear System Theory and Design*, Oxford Series in Electrical and Computer Engineering, Oxford Univ. Press, New York, 1998.

[6] Bartels, R. H., and Stewart, G. W., "Algorithm 432: Solution of the Matrix Equation $AX + XB = C$," *Communications of the ACM*, Vol. 15, 1972, pp. 820–826. doi:10.1145/361573.361582

[7] Moore, B., "Principal Component Analysis in Linear Systems: Controllability, Observability, and Model Reduction," *IEEE Transactions on Automatic Control*, Vol. 26, 1981, pp. 17–31. doi:10.1109/TAC.1981.1102568

[8] Laub, A. J., Heath, M. T., Paige, C. C., and Ward, R. C. "Computation of System Balancing Transformations and Other Applications of Simultaneous Diagonalization Algorithms," *IEEE Transactions on Automatic Control*, Vol. 32, 1987, pp. 115–122. doi:10.1109/TAC.1987.1104549

[9] Lall, S., Marsden, J. E., and Glavaski, S. "A Subspace Approach to Balanced Truncation for Model Reduction of Nonlinear Control Systems," *International Journal of Robust and Nonlinear Control*, Vol. 12, 2002, pp. 519–535. doi:10.1002/rnc.657

[10] Rowley, C. W. "Model Reduction for Fluids, Using Balanced Proper Orthogonal Decomposition," *International Journal of Bifurcation and Chaos in Applied Sciences and Engineering*, Vol. 15, 2005, pp. 997–1013. doi:10.1142/S0218127405012429

[11] Safonov M. G. and Chiang, R. Y. "A Schur Method for Balanced Model Reduction," *IEEE Transactions on Automatic Control*, Vol. 34, No. 7, July 1989, pp. 729–733. doi:10.1109/9.29399

[12] Holmes, P., Lumley, J. L., and Berkooz, G. *Turbulence, Coherent Structures, Dynamical Systems, and Symmetry*, Cambridge Univ. Press, Cambridge, England, U.K., 1996.

[13] Enns, D. F., "Model Reduction with Balanced Realizations: An Error Bound and Frequency-Weighted Generation," *Proceedings of the IEEE Conference on Decision and Control*, IEEE Press, Piscataway, NJ, Dec. 1984, pp. 12–14.

[14] Ma, Z., Ahuja, S., and Rowley, C. W.,"2009 Reduced Order Models for Control of Fluids Using the Eigensystem Realization Algorithm," *Theoretical and Computational Fluid Dynamics*, Springer, New York, 2010.